Journal Pre-proofs

Synthesis and biological evaluation of 9-aryl-1,8-dioxo-octahydroxanthene derivatives as antileishmanial agents

Kamlesh Lodha, Deepak Wavhal, Namdeo Bhujbal, Priyanka Mazire, Sneha Bhujbal, Ashlesha Korde, Kamini Bagul, Amit Roy, Rohan Meshram, Vaishali Shinde

Please cite this article as: K. Lodha, D. Wavhal, N. Bhujbal, P. Mazire, S. Bhujbal, A. Korde, K. Bagul, A. Roy, R. Meshram, V. Shinde, Synthesis and biological evaluation of 9-aryl-1,8-dioxo-octahydroxanthene derivatives as antileishmanial agents, *Results in Chemistry* (2023), doi: https://doi.org/10.1016/j.rechem.2023.100943

This is a PDF file of an article that has undergone enhancements after acceptance, such as the addition of a cover page and metadata, and formatting for readability, but it is not yet the definitive version of record. This version will undergo additional copyediting, typesetting and review before it is published in its final form, but we are providing this version to give early visibility of the article. Please note that, during the production process, errors may be discovered which could affect the content, and all legal disclaimers that apply to the journal pertain.

Synthesis and biological evaluation of 9-aryl-1,8-dioxo-octahydroxanthene derivatives as antileishmanial agents

Kamlesh Lodha[1], Deepak Wavhal[1], Namdeo Bhujbal[2], Priyanka Mazire[3], Sneha Bhujbal[4], Ashlesha Korde[4], Kamini Bagul[4], Amit Roy[3], Rohan Meshram[4*], Vaishali Shinde[1*]

[1]Department of Chemistry, Savitribai Phule Pune University (Formerly University of Pune), Pune 411007, India. Corresponding author email address: vaishali.shinde@unipune.ac.in

[2]Annasaheb Magar College, Savitribai Phule Pune University (Formerly University of Pune), Pune 411007, India.

[3]Department of Biotechnology, Savitribai Phule Pune University, (Formerly University of Pune), Pune 411007, India.

[4]Bioinformatics Centre, Savitribai Phule Pune University, (Formerly University of Pune), Pune 411007, India. Corresponding author email address: rohan@bioinfo.net.in

Abstract

In the current research, we designed and synthesized various derivatives of 9-aryl-1,8-dioxo-octahydroxantheneusing flow chemistry technique and explored *in vitro* study for antileishmanial activity against the promastigote as well as amastigote form of *Leishmania donovani* strain. Among the tested analogs by various cell viability assays, six compounds exhibited antileishmanial activity with IC$_{50}$ value ranging from 24.81 to 52.33 μM. Further, the functional dynamics study sheds light on the structural role of various functional groups presents in the xanthene derivatives for defining the actual antileishmanial activity. Molecular dynamics simulation data presented here attempts to provide a structural and mechanistic explanation of threonine synthase inhibition against *Leishmania donovani* by xanthene derivatives. Described structure-activity-relation advocates for further modification of the xanthene scaffolds for the accomplishment of challenging antileishmanial drugs.

Key words: Antileishmanial activity, Continuous flow chemistry, 1,8-Dioxo-octahydroxanthene, Molecular dynamics simulations, Threonine synthase inhibition.

Introduction

Leishmaniasis is produced by the single-celled intracellular parasite of the genus *Leishmania* and transmitted by sandfly bites. Cutaneous, mucocutaneous and visceral leishmaniasis are endemic in tropical and subtropical areas [1]. Visceral leishmaniasis, also referred to as kala-azar, is a lethal form of leishmaniasis caused by the protozoan parasite, *Leishmania donovani* and communicated by the bite of the vector sand fly, *Phlebotomus argentipes* [2]. More than 90 species of sand flies are known to transmit the leishmanial parasite [3]. It has been reported that visceral leishmaniasis, if left untreated, can lead to 95% fatality or result in post-kala-azar dermal complication [4]. It is estimated that about one

billion individuals are at risk of infection across 98 nations around the world, with over 1.5 million new cases being reported annually and 20,000–40,000 fatalities being recorded every year [5]. Therapy for this significant infectious disease is still limited and relies on a few medications, such as pentavalent antimonial, amphotericin B, and miltefosine [6]. These medications have drawbacks such as severe adverse effects, high prices, and in some situations, diminished efficacy, which can be caused by parasite resistance [7]. Therefore, research on finding newer and effective drugs and identifying novel drug targets is gaining a momentum in parasitology research. The details of newly identified antileishmanial drug compounds at different clinical trial stages along with their drug targets is effectively reviewed by Santana *et al* [8].

In a recent computational subtractive genomic based analysis, our group proposed Threonine Synthase (TS) as an effective antileishmanial drug target [9]. The metabolic simulation data of the threonine biosynthetic pathway presented in the same study demonstrated that inhibition of TS can result in the collapse of amino-acid metabolism in the parasite leading to the desired therapeutic effect. Further, upon structural modelling of TS followed by virtual screening of 44,000 compounds from FilterBase database library, a few challenging putative antileishmanial scaffolds were picked out. All the identified structures consist of two to three cyclic rings connected through two to three atoms length linker chain with amide or ether or ester functional group. Amongst the recognised antileishmanial agents, xanthene scaffold (**5**) is privileged structure as a promising chemical pharmacophore [10]. Xanthene derivatives showed strong effects against axenic amastigotes and intracellular amastigotes of *L. Mexicana* [11]. Xanthone derivative obtained from medicinal plants, *Allanblackia monticola*, and *Symphonia globulifera* given promising antileishmanial activity against *L. donovani* [12]. Xanthene derivatives are also shown good antileishmanial activity against *L. amazonensis* [13].Our objective hereby was to experimentally validate the predictive results obtained in the previous study.

The target threonine synthase from *Leishmania donovani* is a PLP-dependent enzyme belonging to the *ß*-family of PLP-dependent enzymes [14-15]. The structural model of the catalytic domain of leishmanial TS was recently published which indicates the presence of three distinct domains [10]. The active site of the TS is present near the PLP binding site. The residues lining of this site are mostly basic for the electrostatic trapping of the negatively charged PLP prosthetic group and successful catalysis. The enzyme functions by the formation of covalently bound internal and external aldimine complexes [10]. There are four structurally and functionally conserved motifs found in Leishmanial TS active site. The asparagine loop also called motif-1 is generally involved in substrate-induced structural rearrangements. Motif-2 corresponds to a high-flexibility loop involved in substrate recognition. Motif-3 is called a phosphate binding loop and motif 4 is termed the PLP binding region [10] (Figure-S7 in Supplementary material).All these regions orchestrate a successful catalysis event.
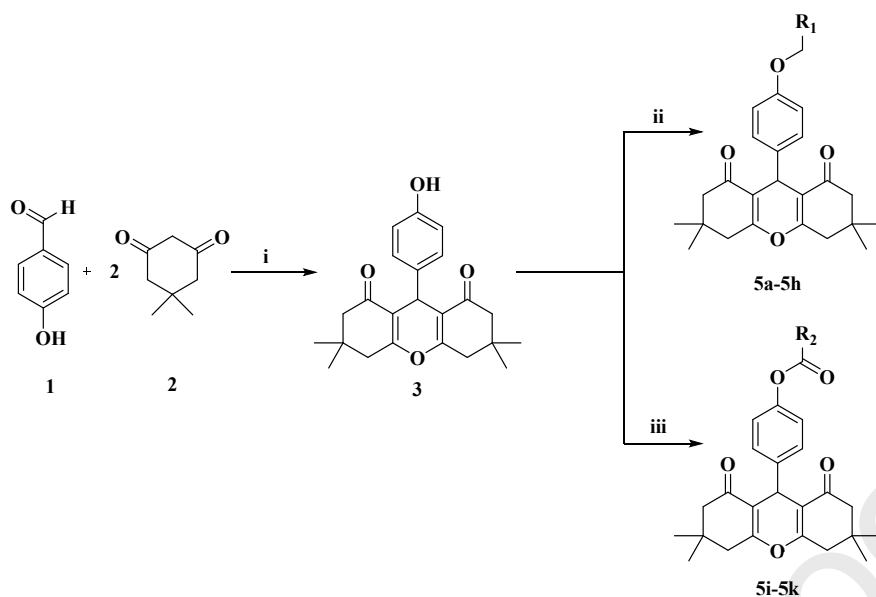
Xanthene scaffold is found in natural compounds such as Gaudichaudione A, Gaudichaudione B, Allanxanthone C, and Funiculosone (Figure-1) [16-19].
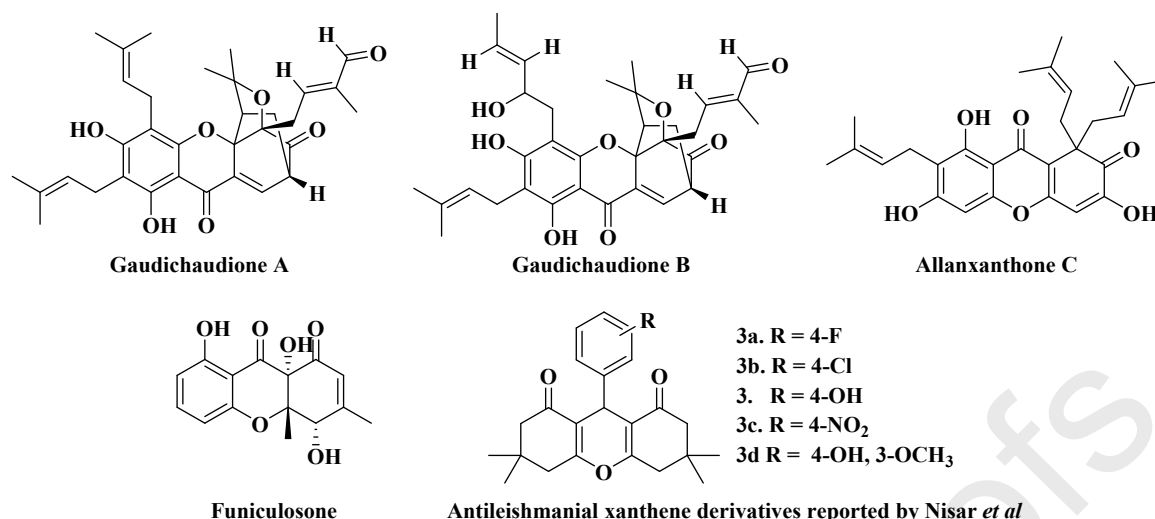
Figure-1: Chemical structures of some bioactive compounds having xanthene scaffold

Xanthene core is also established to have many medicinal applications such as anti-bacterial and anti-fungal [20], anti-inflammatory [21], analgesic [22], antineoplastic [23-24], membrane receptor antagonist [25], phototoxic in microorganisms [26], radical scavenging activity [27], vasorelaxing, antihypertensive activity [28] and antitubercular activity [29] to mention a few. In terms of parasitic research, xanthene compounds are demonstrated as an effective antimalarial agent [30]. Chibale *et al* demonstrated that xanthene compounds arrest the growth of *Trypanosoma cruzi*, a parasite responsible for African sleeping sickness by inhibiting enzyme trypanothione reductase [31]. The elementary antileishmanial activity of 9-aryl-1,8-dioxo-octahydroxanthene analogs was proposed by Nisar *et a l* (Figure-1), but their study was limited to model organism *Leishmania major* and it was shown that the substitution at the para position of the aryl ring might be responsible for antileishmanial activity [32].

Xanthene derivatives are reported to be synthesized by various methods [33, 34] which involves condensation of aldehydes with 5,5-dimethyl-1,3-cyclohexanedione or 1,3-cyclohexanedione. Most of the reported methods include the use of strong protonic acids as a catalyst, toxic reagents and solvents [35-37]. The major drawbacks associated with the reported methods were longer reaction time, high temperature, difficulty in isolation of product and non-feasibility for scaling up for manufacturing [36, 38, 39].

Scheme-1: Synthesis of titled compounds **5a** to **5k**, Reagents and conditions: (i) Ethylene glycol, 100ºC (Flow chemistry) (ii) R_1-CH_2-X (**4a-4h**), acetone, K_2CO_3, 16 to 24 h, (iii) R_2-CO-Cl (**4i-4j**), dichloromethane, triethylamine, 8 to 16 h.

In continuation of our work towards the development of biologically active molecules [40-45], we designed and synthesized the xanthene derivatives using catalyst free reaction conditions as shown in (Scheme 1). Compound **3** was obtained using modern technique flow chemistry with easy isolation and further used as a key precursor for the synthesis of designed target molecules. In the present work, we have synthesized two different series of the 9-aryl-1,8-dioxo-octahydroxanthenederivative with alkoxy or acyloxy linker group at the para position of the aryl ring. All newly synthesized molecules were tested for their *in vitro* antileishmanial activity against *Leishmania donovani*. Additionally, we performed molecular dynamics simulations to gain insights into the structural aspects of the xanthene-based inhibition of promastigotes and amastigotes stages in *Leishmania donovani*.

Results and discussion

Chemistry

We synthesized target molecules consisting of xanthene pharmacophore **3**, linked with different substituted aromatic rings through the alkoxy or acyloxy group. Xanthene moiety was prepared from 4-hydroxybenzaldehyde **1** and dimedone **2** at 100 ºC by using continuous flow chemistry (Scheme 1). The flow chemistry or continuous process is an advance technique, which is fascinating more synthetic chemist for development of more efficient and cost effective process. Flow chemistry technique has more advantage over conventional method, such as, occupy less space, lower equipment cost, high-throughput,

faster reaction, hazardous reaction can be handled easily, etc. For synthesis of **3**, Plug flow reactor (PFR) has been used and in this one-pot reaction might have taken place which includes Knoevenagel condensation, Michael addition, and cyclodehydration in flow reactor to get the desired compound **3** which was isolated by filtration with quantitative yield. Compound **3** was treated with different alkylating and acylating agents to obtain **5a-5k** by nucleophilic substitution reaction. Products were confirmed by ^{1}H-NMR,^{13}C-NMR, and HRMS techniques.

Compound **3** was treated with different alkyl halides (**4a-4h**) in presence of K_2CO_3 at room temperature to furnish **5a-5h** in 78 to 88 % yields.^{1}H-NMR showed the disappearance of broad singlet due to phenolic -OH proton at δ 6.1 and appearance of -CH_2- protons at δ 4.55–5.19 of **5a-5h**. The structures of the target compounds were confirmed by the appearance of additional protons coming from corresponding **4a-4h** at the expected range of chemical shift in ^{1}H-NMR.

In another set of reactions, **3** was treated with acyl chloride (**4i-4k**) and triethylamine at room temperature to obtain **5i-5k** in 66 to 70 % yields. The peak at 1714 to 1720 cm^{-1} in IR spectra due to stretching of carbonyl group confirmed the formation of the ester group. Disappearance of broad singlet due to phenolic -OH proton in ^{1}H NMR confirmed the formation of **4i-4j**. Peak at δ 160 to 161 ppm in ^{13}C NMR confirmed the carbonyl carbon of the ester group.

Biological assays

Anti-promastigote activity:

Among the 12 different compounds screened for their leishmanicidal activity, compounds **5j**, **5i** and **3** demonstrated comparatively effective antileishmanial activity by inhibiting the growth of *Leishmania donovani* promastigotes. Summary of *in vitro* viability assay is shown in Figure-2. A significant difference in viability percentages of promastigotes was observed for different concentrations of compounds **5j**, **5i,** and **3**, which is time dependent manner. Viability of 10.29 %, 10.79 % and 9.22 % were observed respectively after treatment of compounds **5j**, **5i,** and **3** at a concentration of 200 μM for 72 h. The IC_{50} values of compound **5j**, **5i,** and **3** were calculated to be 28.21 μM, 28.08 μM, and 24.81 μM, respectively.
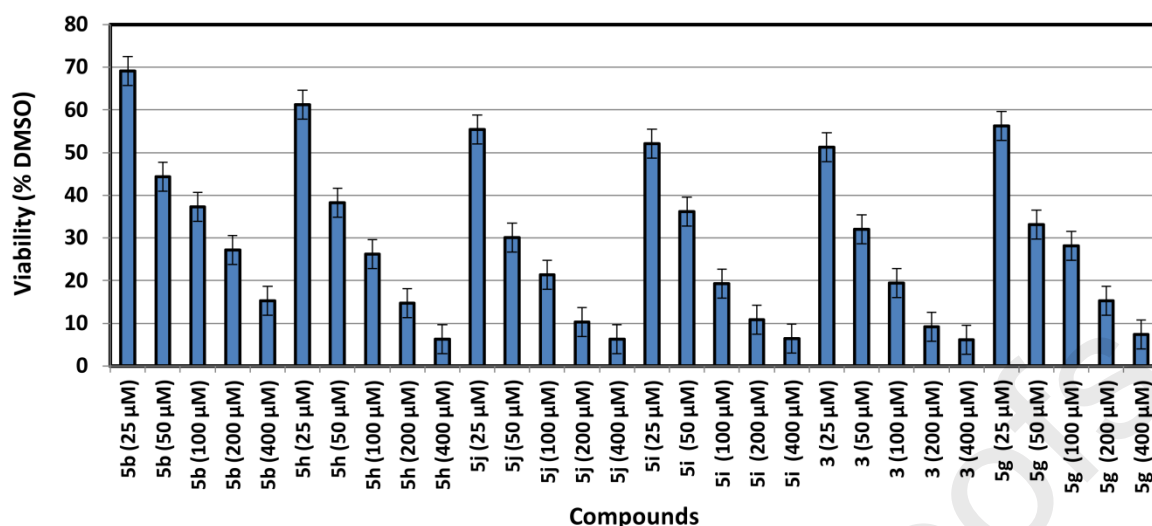
Figure-2: Antileishmanial activity of the synthesized compounds against *L. donovani* promastigotes.

Compounds **5i** and **5j** possesses methyl substituted thiophene group, while **5k** is a thiazole substituted product. It is to be noted that the methyl substituted thiophene group exhibited better antileishmanial effect than that of thiazole containing **5k**. Additionally, the carbonyl functional group (in **5h**) and the ester group (in **5g**) appears to induce the antileishmanial effect. It is to be noted that derivatives **5j**, **5i**, and **3** have demonstrated good antileishmanial effect as compared to amphotericin B (AmB) [46].

Cytotoxicity of compounds:

To assess the cytotoxic effect of the compounds on THP-1 macrophages, cells were treated with compound **5j**, **5i** and **3** (25 and 50 μM) for 72 h and cell viability was assessed by MTT method. The CC_{50} and SI values were calculated for the test compounds which are summarized in Table 1. The percentage of viable THP-1 cells treated with the test compounds was significantly high compared to positive control AmB. It was observed that the cell viability decreased with higher concentration of the compounds (Figure-3). More than 80% cell viability was rendered by compound **3** (25 μM) with an IC_{50} of 28.25 ± 1.9, CC_{50} value of 88.28 ± 0.78 μM and selectivity index (SI) value of 3.1. Besides, in comparison to control drug, compounds **5j** and **5i** (25 μM) also showed higher THP-1 cell viability (80%).

6
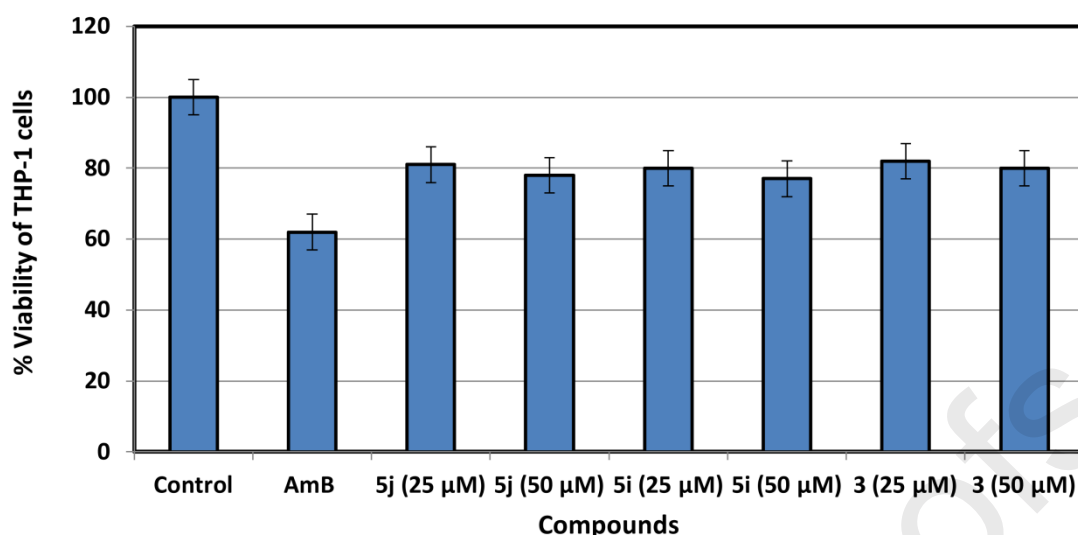
Figure-3: Cytotoxicity of compounds in THP-1 cells by MTT assay.

**Table-1:** Cytotoxicity of compounds using THP-1 cells

Compounds	IC$_{50}$ for promastigotes (µM)	IC$_{50}$ for amastigotes (µM)	CC$_{50}$ (µM)	SI
AmB	4.9 ± 0.74	2.5 ± 1.3	105.88± 3.5	42
5j	28.21 ± 3.2	35.8 ± 0.7	106 ± 1.29	3.0
5i	28.08 ± 2.66	34.36 ± 2.1	101 ± 4.5	2.9
3	24.81 ± 1.9	28.8 ± 0.4	88.28 ± 0.78	3.1

To assess the cytotoxic effect of the compounds on THP-1 macrophages, cells were treated with compounds **5j**, **5i** and **3** (25 and 50 µM) for 72 h and cell viability was assessed by MTT method. The IC$_{50}$ values for promastigotes and amastigotes, CC$_{50}$ and SI values were calculated for the test compounds which are summarized in Table 1. The percentage of viable THP-1 cells treated with the test compounds was significantly high compared to positive control AmB. It was observed that the cell viability decreased with higher concentration of the compounds (Figure-3). More than 80 % cell viability was rendered by compound **3** (25 µM) with an IC$_{50}$ of 28.25 ± 1.9, CC$_{50}$ value of 88.28 ± 0.78 µM and selectivity index (SI) value of 3.1. Besides, in comparison to control drug, compounds **5j** and **5i** (25 µM) also showed higher THP-1 cell viability (80%).

Anti-amastigote activity:

In vitro antiamastigote activity of test compounds were tested by infecting the *L. donovani* promastigotes in differentiated THP-1 cells (Figure 4). AmB was selected as the reference drug for comparison. It was observed that the three compounds **5j**, **5i** and **3** also had substantial anti-amastigote activity with IC_{50} values of 35.8 ± 0.7, 34.36 ± 2.1 and 28.8 ± 0.4 µM, respectively (Table-1). Among the three test compounds, percentage of infectivity was 43 and 30 when amastigotes were treated with compound **3** at a concentration of 25 and 50 µM, respectively. The IC_{50} value for the control drug AmB was 2.5 ± 1.3 µM.
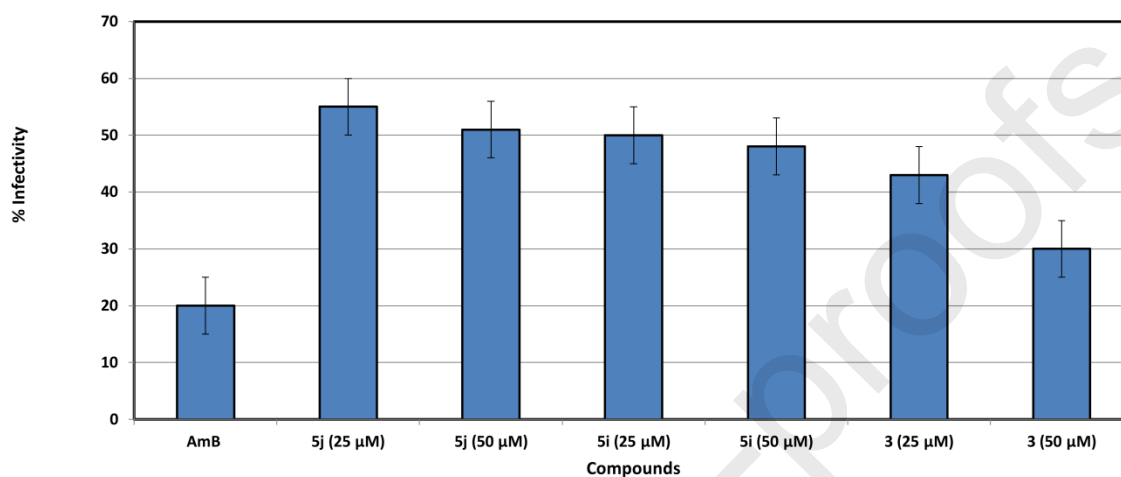
Figure-4: Antileishmanial activity of the compounds against *L. donovani* amastigotes.

In silico analysis

Structural reasoning behind the xanthene induced antileishmanial effect has been very rarely discussed in the literature. Additionally, to associate the experimental observations and to account for structural logic behind xanthene based TS inhibition, we took up an *in silico* approach. We initially performed molecular docking to obtain the TS-xanthene complexes. Results from docking yield a rather static representation of the protein ligand system [47]. Generally, at cellular conditions, biological macromolecules including enzymes are in a continuous dynamic state and it is believed that its dynamics dictate the enzyme activity as well as inhibition [48]. Therefore, the time dependent conformational changes that happen during enzyme inhibition may be missed in such an elementary analysis. Thus, to monitor dynamic interactions of xanthene ligands into the active site of TS, we performed MD simulations using NAMD.

RMSD and RMSF

Plotting the RMSD of protein atoms during the simulation enables us to know if the TS-xanthene complexes attained conformational stability. RMSD is often considered an indicator of system convergence towards an equilibrium state. A molecular system is

assumed to be converged when the RMSD of the protein-ligand system does not fluctuate intensely and become stable around a fixed value when the simulation ends. Typically, when the RMSD values start to get recorded in a plateau with the range of 1-3 Å, such behaviour acts as an indication of system convergence and attainment of conformational stability for the protein ligand system. Supplementary Figure-S1 corresponds to the trend of RMSD observed for all 12 protein-ligand complexes simulated for 25 Ns timespan in this study. It is clearly evident that for all compounds except **5i**, a stable plateau of RMSD is reached after about 10 Ns of the simulation where most of the protein ligand complexes converge around the value of 2 to 3 Å. This observation indicates system stability in the TS-xanthene system. In the case of compound **5i**, it is observed that its complex with TS attained convergence at a higher RMSD value after 15 Ns. Such a trend indicates that the remaining ligands have more stability of ligand with the enzyme.

RMSF analysis is conducted to monitor the flexibility of residues in the protein along the course of the simulation trajectory. Higher values for RMSF are an indication of the higher level of displacement of a residue from an average position. Therefore, higher stability is attributed to lower values of RMSF [49]. As observed in Supplementary Figure-S1, residues 258-261 form the roof of PLP, while residues 289-296, 474-476, 555-556 lines the ligand binding pocket and residues ranging from 419-425 form the surface for PLP site, in the *Leishmania donovani* TS. Interestingly, these residues show a lower degree of RMSF indicating that these regions are more stable in the protein-ligand complexes during the course of the simulation. The RMSF pattern in residues obtained here is in accordance with that for previously reported TS in *Leishmania major* [10].

The binding free energy of the compounds obtained from the MMPBSA method is summarized in Table 2.

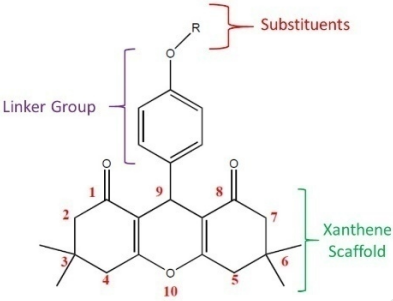**Table 2**: Summary of the MMPBSA free energy calculations

Compounds	Δ Electrostatic interaction	Δ Van der Waal force	Δ Poisson Boltzmann	Δ surface area	Δ Gas phase energies	Δ Solvation free energy	Δ Polar interactions	Δ Non Polar interactions	Total Free Energy ΔG
3	-20.5± 4.0	-49.3± 3.2	71.3± 5.1	-7.1± 0.2	-69.8± 5	64.2± 5.1	50.8± 4.2	-56.4± 3.3	**-5.5± 4.8**
5a	-0.2± 6.7	-42.3± 2.9	42.5± 6.9	-6.1± 0.1	-42.6± 7	36.3± 6.8	42.2± 5.3	-48.5± 3	-6.2± 4.3
5b	-2.3± 5.5	-28.2± 2.4	24.9± 7.1	-5.3± 0.2	-30.6± 6.2	19.5± 7	22.5± 3.8	-33.6± 2.6	**-11.0± 2.8**
5c	-324.0±44.9	-20.9± 4.4	337.5± 43.6	-4.4± 0.2	-344.9±45.6	333± 43.4	13.5± 8	-25.3± 4.5	-11.8+ 6.7
5d	2.6± 5	650.9± 19.5	40.2± 3.8	-6.9± 0.1	653.5± 20.5	33.2± 3.8	42.8± 3.4	643.9± 19.6	686.8± 19.9
5e	-11.5± 4.5	-32.0 ± 4.2	36.4 ± 10.8	-4.8± 0.3	-43.6± 7.7	31.5 ± 10.6	24.8± 8	-36.9 ± 4.5	-12 ± 6.5

5f	-6.2 ± 6.1	-24.8 ± 4	18.8 ± 8.6	-4 ± 0.3	-31.1± 9	14.7± 8.4	12.5± 5.2	-28.9 ± 4.4	-16.3± 5.4
5g	-14.7± 5.2	-44.9± 3.9	49.9± 6.4	-6.6± 0.3	-59.7± 6.6	43.3± 6.2	35.1± 3.9	-51.5± 4.2	**-16.4± 2.9**
5h	-9.8± 5.6	-42± 3.3	50.1± 6.7	-5.6± 0.2	-51.9± 7	44.4± 6.6	40.2± 4	-47.7± 3.5	**-7.5± 3.2**
5i	-31± 1.5	38.5± 3.2	-30.2± 0.8	4.8± 0.05	7.4± 3.3	-25.4± 0.8	-61.3± 1.5	43.3± 3.1	**-17.9± 3.4**
5j	-11.3± 3.9	-43.7± 2.6	53.2± 5.6	-6.5± 0.2	-55± 4.6	46.7± 5.6	41.9± 5.1	-50.2± 2.8	**-8.3± 5.5**
5k	-4.5± 4.4	673.4± 21.4	26± 4.8	-5.1± 0.5	668.8± 21.5	20.9± 4.5	21.6± 3.9	668.2± 21.5	689.8± 21.1

The data expressed above for different terms in MMPBSA free energy estimation was collected from final 100 frames of the trajectory. Therefore, values above are mean± sd for last 100 frames. The numbers are limited to one decimal precision as reported in the log file obtained from the CaFE software.

Interactions observed in the representative pose of the cluster analysis of the MD simulation trajectories are summarized in Table 3.

Table 3: Summary of the interactions observed in the representative pose of the cluster analysis of the MD simulation trajectories.

Compound		
	HB Pair (HB Distance)	**Apolar (Van der Waal's and hydrophobic) contacts**
3	Asn-579::(O^{bb}) :: Lig(Lnk):O [2.97]	Gln474, Pro474, Ans447, Pro555, Gly291, Asp584, Thr578, Ser583, Ala258, Leu577, Asp292, PLP, Ser290, Asn379, Ser475, Ile476
5a	Arg-551:(N^{sc}):: Lig(Sub):O[3.16] Arg-551:(N^{sc}):: Lig(Sub):O[2.61]	Leu552, Thr578, Asp584, PLP, Gly291,Ser583, Ser290, Ser475, Asn422, Ile476, Pro474, Gln448,His556, Asp554
5b	No interaction	Ala288, Ile476, Gln349, Phe345, Ser320, Ser472, Ser473, PLP, Ile478, Pro474
5c	Asn-447:(N^{sc}):: Lig(Xan):(O) [3.06]	Ser473, Gly421, Asn422, Asp554, Ser583, Leu552, Asn579, Leu553, Thr578, Pro580, Thr585, Pro555, Ile478, Gln448, Ser472, Ile476, Pro474, Asn449
5d	His-556:(N^{sc})::Lig(Xan):(O) [2.75]	Asn379, Thr293, Gly421, Pro474, Ile476, Gln448, Ser473,Ser472, Thr585, Thr578, Ser583, Asn579
5e	No interaction	Ser473, Gln448, His556, Asn449,

12

		Ser446, Pro474, Arg466, Ile476, PLP, Ser472, Phe345
5f	No interaction	Asn379, Thr293, Gly421, Pro474, Ile476, Gln448, Ser473,Ser472, Thr585, Thr578, Ser583, Asn579
5g	Ser-290:(OG^{sc}):: Lig(Sub):(O) [2.76] Ser-472:(N^{bb}):: Lig(Sub):(O) [2.85]	Pro474, Thr578, Leu577, Asp554, PLP, Pro555, Gly381, Met316, His317, Pro315, Thr471, Phe345
5h	Thr-578: (OG1^{sc}):: Lig(Sub):O[2.56]	Gln323, Val295, Asp292, Pro555, Asp554, Ile540, Asp584, Ser472, Ser583, Ser473,Ser475, Pro474, Ser582, Gly291,
5i	No interaction	Ile476, Ser475,Gln448, Pro474, Asn447, Plp, Asp292, Asn579, Pro580, Gly291,Ser290, Asn379, Pro555
5j	No interaction	Gly421, Plp, His556, Ile478, Asp292, Thr256, Ala258, Val295, Ser582, Thr578, Pro555, Gln448, Asn447, Asn442
5k	Ser-583:(OG^{sc}):: Lig(Sub):(O) [2.70]	Thr289, His556, Ser475, Gln448, Pro474, Pro555, Pro580, Asp584, Thr578, Asn579, Asp554

It can be observed that compounds with the decent *in vitro* activity correlates with the negative free energy values. For example, compound **5i** with the most promising *in vitro* activity (28.08 μM) also demonstrated better binding free energy value (-17.9 Kcal/mol) (Table 3). Similar observation was made in the case of compound **5g**. Similarly, compound **5d** and **5k** performed poorly in *in vitro* testing on promastigotes (they failed to show positive results in the viability assay) and correspondingly they scored positive values in the binding free energy calculations. The results for compounds like **3** and **5j** seem to be puzzling because they appear to possess better *in vitro* activity (24.81 and 28.21 μM respectively) but have comparative higher binding free energy values (-5.5 Kcal/mol and -8.3 Kcal/mol respectively) as compare to the best performing compounds (-17.9 Kcal/mol). On the other hand, compound **5b** scored one of the best binding free energy score (-11 Kcal/mol) but did not performed well in experimental assay (IC$_{50}$ value of 52.33). These discrepancies might arise due to the limitation of the molecular dynamics methodology discussed as follows.

13

Firstly, in the current study, the free energy estimation was performed using the MMPBSA method. MMPBSA method ignores the entropic contribution in the free energy estimation and thus might sometimes result in differential free energy values (**Supplementary material**). Secondly, during the MD simulation, the initial velocity values are randomly assigned from the Maxwell-Boltzmann distribution to initiate the Velocity Varlet integration algorithm for propagating the system in time. Therefore, owing to the stochastic involved in the technique, the differential initial velocities might sometimes affect the final free energy calculation. Moreover, compounds **5b**, **5i**, **5j** that recorded better *in vitro* antileishmanial activity appear to lack polar contacts in the form of hydrogen bonds in the cluster analysis results. This fact points out that non polar interactions in the form of van der Waal's contacts and hydrophobic interactions might play a dominating role in shaping the xanthene induced antileishmanial activity. Such nonpolar contribution can be attributed to the two cyclic rings and four methyl groups at the third and sixth positions on the xanthene ring. MD simulations revealed that interaction of the ligand with residue Ser-290 might be mediated through ester substituent rather than the linker oxygen as predicted in the initial docking study. Moreover, MD simulations of compound **5g** revealed that polar interaction with Ser-472 from TS might be involved to stabilize the protein-inhibitor complex that was not detected in the initial docking study. The results obtained from the clustering of MD simulation data identified that the oxygen of the carbonyl functional group from compound **5h** at its substituent position may form a stable hydrogen bond with the side chain of Thr-578 rather than the oxygen from the prosthetic group as predicted in the docking result (supplementary material Figure S4 B).The detailed discussion of the dynamic interactions of xanthene compounds with the residues from TS and their functional impacts can be found in the supplementary material.

Conclusions

Herein we reported the design and synthesis of some 9-aryl-1,8-dioxo-octahydroxanthene derivatives. This report validates the prediction that 9-aryl-1,8-dioxo-octahydroxanthene can indeed act as an effective antileishmanial pharmacophore by inhibiting the parasite TS. Along with parent compound **3**, derivatives (**5i**, and **5j**) showed comparable antileishmanial effect. Data obtained from the binding free energy and structural data from MD simulations also advocates the fact that bulkier functional groups may deter the antileishmanial activity of xanthene moiety and low molecular weight functional groups if used may contribute to the improvement of the existing 9-aryl-1,8-dioxo-octahydroxanthene parent compound.

Experimental Section

Chemistry:

Synthesis of 9-(4-hydroxyphenyl)-3,3,6,6-tetramethyl-3,4,5,6,7,9-hexahydro-1H-xanthene-1,8(2H)-dione (3).

A solution of compound **1** (2.73 M, 1.0 equiv.) in ethylene glycol (flow rate: 0.5 mL/min) and a solution of compound **2** (2.38 M, 2.02 equiv.) in ethylene glycol (flow rate: 1.2 mL/min) were introduced to T-shaped mixer (inner diameter: 1.0 mm) at temperature 100 ºC with the peristaltic pumps. The resulting mixture was passed through plug flow reactor (PFR) (inner diameter: 2.0 mm, length: 3.2 m, volume: 10 mL, reaction time: ~ 6 minutes) at the same temperature. Then, the resulting mixture was collected and cooled to room temperature under stirring and filtered to get pure compound **3** with 97 % yield and 99 % purity by HPLC as a pale-yellow powder. M.P. 249 ºC (reported: 246-248 ºC) [34].FTIR

(cm^{-1}): 3367, 2959, 1655, 1614, 1357, 1200, 1157, 835. ^{1}H-NMR (400 MHz, CDCl$_3$) δ 7.11 (d, J = 8.4 Hz, 2H), 6.60 (d, J = 8.4 Hz, 2H), 4.69 (s, 1H), 2.48 (s, 4H), 2.23 (q, J = 16.3 Hz, 4H), 1.11 (s, 6H), 1.02 (s, 6H).^{13}C-NMR (100 MHz, CDCl$_3$) δ 196.98, 162.30, 154.47, 135.94, 129.41, 115.88, 115.18, 50.79, 40.88, 32.25, 30.98, 29.20, 27.39. HRMS (ESI) m/z calculated for C$_{23}$H$_{26}$O$_4$ [M+H]$^+$: 367.1831, found: 367.1833.

General procedure for synthesis of compounds 5a-5h

A solution of **3** (2.73 mmol) and **4** (2.73 mmol) in acetone (10 mL) was stirred with K$_2$CO$_3$ (6.83 mmol) at room temperature for 16 to 24 h. After completion of the reaction (monitored by TLC) the mixture was filtered and purified by silica gel column chromatography (78-88 % yield).

General procedure for synthesis of compounds 5i-5k:

To a solution of compound **3** (2.73 mmol) in dichloromethane (20 mL), the solution of triethylamine (4.1 mmol) and **6** (2.73 mmol) in dichloromethane (10 mL) was added drop wise at room temperature. The reaction mixture was stirred for 8 to 16 h. After completion (monitored by TLC) the reaction mass was quenched with 10 % hydrochloric acid till pH 7. The organic layer was separated, dried over Na$_2$SO$_4$ and purified by silica gel column chromatography (66-70 % yield).

Biological assays

The cytotoxicity of the compounds was determined by MTT assay. Briefly, in 96-well microtitre plate, *Leishmania donovani* AG83 promastigotes (2 x 10^{60}cells) were cultured in M-199 medium supplemented with 10% heat inactivated fetal bovine serum and allowed to multiply for 72 h in the medium alone or in the presence of different compounds at 25 °C. After incubation, 5 mg/mL MTT solution was added to the promastigotes in each well and incubated for 3 h at 25 °C. After incubation period cells were centrifuged at 1000 g for 10 min, the supernatant was discarded and 100 μL of DMSO was added to each well and resuspended. The yellow tetrazolium MTT dye is reduced to insoluble formazan crystals (purple colour) in living cells using NADH as a reducing agent. The colorimetric data of absorbance is measured at 570 nm by multi-mode plate reader. The percentage viability and IC$_{50}$ values were calculated. The experiments were performed three times and an average of three experimental data is expressed as mean ± SD.

Experimental infection of macrophages with *L. donovani* parasites:

THP-1 cells were allowed to differentiate to mature macrophage and become adherent with phorbol 12-myristate 7-acetate (PMA) (20nM) for 12 h. The non-adherent cells were removed by washing with RPMI without FBS. The cells were then infected with *Leishmania* parasite for 24 h at parasite-macrophage ratio of 10:1. The unbound parasites were removed by washing with PBS (1 X) and were further incubated for 48 h at 5 % CO$_2$. The macrophage cells were then treated with different concentrations of compounds (**5i**, **5j** and **3**) and AmB (1μM) for 72h. Post- treatment the macrophages were fixed and stained with May-Grunwald-

15

Giemsa Stain. The parasite load was measured by counting the number of amastigotes per 100 macrophages. Percent amastigote infectivity was determined by

$$\% \text{ Infectivity} = \frac{\text{Number of amastigotes per 100 macrophage (treated sample)}}{\text{Number of amastigotes per 100 macrophage (infected control)}} \, X \, 100$$

IC_{50} was determined by graphical extrapolation. Each measurement was performed in triplicate and the data were expressed as mean ± SD.

In vitro cytotoxic effect of the compounds

Cell viability was measured by MTT assay to observe the cytotoxicity of the compounds (**5j**, **5i** and **3**) and 1µM AmB as a positive control using human macrophage cells (THP-1). PMA-differentiated THP-1 cells were maintained in RPMI-1640 medium (10 % FBS) and treated with test compounds (25 and 50 µM) for 72 h. The cells with only media served as the negative control. The supernatant was then removed, and 50 µL of RPMI-1640 medium containing 0.5% *w/v* MTT was added and incubated for 3h. Finally, 200 µL of DMSO was added to solubilize the insoluble MTT product. The microplate spectrophotometer was used for colorimetric analysis at 540 nm wavelength. The absorbance at the given wavelength, and the readings were used to quantify cytotoxic effects in terms of CC_{50}. Each test was performed in triplicate, and the results were expressed as mean ± SD.

Computational studies

Molecular docking: Molecular Docking was performed as per a well-established protocol published elsewhere [50]. AutoDock [51,52] was used for molecular docking that was embedded in a python-based GUI PyRx [53]. The grid box of default size was placed around the covalently attached PLP group in the protein coordinate file. All the remaining docking parameters were set to default.

MD simulation: The protein-ligand complexes obtained in molecular docking were used in subsequent MD simulations. MD simulations were performed to monitor the functional dynamics involved in the ligand binding site of TS. Moreover, advanced endpoint analysis techniques for free energy estimation require trajectories data from MD simulations. Prior to MD simulations, the topologies and parameters for xanthene compounds were obtained from Match Server [54]. MD simulations were conducted for each protein ligand complexes using the protocol established in our lab [55]. Briefly, all MD simulations were performed as conventional MD simulations that involve processes like minimization, heating, equilibration followed by production runs. NAMD was used to perform all MD simulations using CHARMM forcefield [56]. Long range interactions were evaluated using the switching function. The parameters in the switching function like switching distance and cut off were set to 8 and 12 Å respectively. The Shake algorithm was used to manage the constraints between hydrogen and heavy atoms [57]. The electrostatic forces in the system were evaluated using the Particle Mesh Ewald (PME) method [58]. The minimization step was completed by using 4000 steps of the conjugate gradient algorithm. In the subsequent heating phase that lasted for 300 ps, the temperature of the system was increased by 0.001 K at each integration step and simultaneously the velocities were reassigned. Thus, in the heating step

the temperature of the system was gradually increased from 0 to 300 K. Equilibration simulation of 1 Ns was conducted to obtain the thermodynamically stable state of the system. Equilibration was performed in the NPT ensemble state where the temperature was controlled using the Hoover thermostat [59] and pressure was maintained using the Langevin piston method [60, 61]. Finally, a 25 ns production run was performed for each TS-xanthene derivative complex using a 2 fs time-step. The dynamic and structural properties of the TS-xanthene derivative complexes were sampled from the frames obtained from the production run.

Trajectory analysis and free energy estimations

Trajectory analysis like RMSD, RMSF was conducted using VMD. Cluster analysis was performed usingtheg_cluster command from the Gromacs package. The free energy estimations were performed using the endpoint method applying the MMPBSA methodology. MMPBSA calculations were performed using the Calculation of Free Energy (CaFE) plugin [62]. Details of the procedure are provided in the supplementary information.

Limitations of the study and further work: The current work was aimed to synthesize the series of xanthene analogues and test if they have antileishmanial activity. Inspired from the encouraging results obtained here, we now aim for cloning and over expressing TS from *Leishmania donovani*. The cloning and expression of TS is underway and we hope to test the compounds on the purified TS enzyme.

Supplementary material summary

The supplementary material contains the detailed characterization data of the synthesized compounds along with the NMR Spectra. Detailed mathematical expressions and their explanation is provided for computational methodology part. The details of interaction analysis observed in MD simulations is also made available in the supplementary material.

Declaration of competing interest

The authors declare that they have no known competing financial interests or personal relationships that could have appeared to influence the work reported in this paper.

Acknowledgments

References

1. S. Burza, S. L. Croft, M. Boelaert, *Lancet.* **2018**, *392*, 951–970.
2. O. P. Singh, P. Tiwary, A. K. Kushwaha, S. K. Singh, D. K. Singh, P. Lawyer, E. Rowton, R. Chaubey, A. K. Singh, T. K. Rai, M. P. Fay, J. Chakravarty, D. Sacks, S. Sundar, *Lancet Microbe* **2021,** *2*, e23-e31.
3. WHO Report 2021, https://www.who.int/news-room/fact-sheets/detail/leishmaniasis (Accessed 20th September 2021).
4. G. Grifferty, H. Shirley, J. McGloin, J. Kahn, A. Orriols, R. Wamai, *Res. Rep. Trop. Med.* **2021**, *12*, 135-151.

5. H. Ashwin, J. Sadlova, B. Vojtkova, T. Becvar, P. Lypaczewski, E. Schwartz, E. Greensted, K. Van Bocxlaer, M. Pasin, K. S. Lipinski, V. Parkash, G. Matlashewski, A. M. Layton, C. J. Lacey, C. L. Jaffe, P. Volf, P. M. Kay, *Nat. Commun.* **2021**, *12*, 215.

6. L. F. D. Passero, E. D. S. Brunelli, T. Sauini, T. F. A. Pavani, J. A. Jesus, E. Rodrigues, *Front. Pharmacol.* **2021**, *12*, 690432.

7. J. A. Jesus, I. M. O. Sousa, T. N. F. da Silva, *Pharmaceutics.* **2021**, *13*, 908.

8. W. Santana, S. S. C. de Oliveira, M. H. Ramos, A. L. S. Santos, S. S. Dolabella, E. B. Souto, P. Severino, S. Jain, *Chem. Biodiversity*. **2021**, *18*, e2100336.

9. R. J. Meshram, M. B. Goundge, B. S. Kolte, R. N. Gacche, *Parasitol. Int.* **2019**, *69*, 59–70.

10. R. J. Meshram, K. T. Bagul, S. U. Aouti, A. M. Shirsath, H. Duggal, R. N. Gacche, *Mol. Diversity.* **2021**, *25*, 1679-1700.

11. C. F. M. Silva, D. C. G. A. Pinto, P. A. Fernandes, A. M. S Silva, *Pharmaceuticals.* **2022**, *15*, 148.

12. B. Lenta, C. Vonthron-Sénécheau, B. Weniger, K. Devkota, J. Ngoupayo, M. Kaiser, Q. Naz, M. Choudhary, E. Tsamo, N. Sewald, *Molecules.* **2007**, *12*, 1548–1557.

13. A. G. B. Azebaze, B. M. W. Ouahouo, J. C. Vardamides, A. Valentin, V. Kuete, L. Acebey, V. P. Beng, A. E. Nkengfack, M. Meyer, *Chem. Nat. Compd.* **2008**, *44*, 582–587.

14. M. Garrido-Franco, S. Ehlert, A. Messerschmidt, S. Marinkovic, R. Huber, B. Laber, G. P. Bourenkov, T. Clausen, *J. Biol. Chem.* **2002**, *277,* 12396-12405.

15. F. W. Alexander, E. Sandmeier, P. K. Mehta, P. Christen, *Eur J Biochem.* **1994**, *219,* 953-960.

16. O. Chantarasriwong, B. D. Althufairi, N. J. Checchia, E. A. Theodorakis, *Stud. Nat. Prod. Chem.* **2018**, *58*, 93-131.

17. A. G. Azebaze, M. Meyer, A. Valentin, E. L. Nguemfo, Z. T. Fomum, A. E. Nkengfack, *Chem. Pharm. Bull.(Tokyo).* **2006**, *54,* 111-113.

18. X. M. Gao, T. Yu, F. S. Lai, Y. Zhou, X. Liu, C. F. Qiao, J. Z. Song, S. L. Chen, K. Q. Luo, H. X. Xu, *Bioorg. Med. Chem.* **2010**, *18*, 4957-4964.

19. S. Padhi, M. Masi, A. Cimmino, A. Tuzi, S. Jena, K. Tayung, A. Evidente, *Phytochemistry.* **2019**, *157*, 175-183.

20. M. Kaya, E. Basar, F. Colak, *Med. Chem. Res.* **2011**, *20*, 1214–1219.

21. J. P. Poupelin, G. Saint-Ruf, O. Foussard-Blanpin, G. Narcisse, G. Uchida-Ernouf, R. Lacroix, *Chem. Informationsdienst.* **1978**, *13*, 67–71.

22. H. N. Hafez, M. I. Hegab, I. S. Ahmed-Farag, A. B. el-Gazzar, *Bioorg. Med. Chem. Lett.* **2008**, *18*, 4538-4543.

23. N. Mulakayala, P. V. Murthy, D. Rambabu, M. Aeluri, R. Adepu, G. R. Krishna, C. M. Reddy, K. R. Prasad, M. Chaitanya, C. S. Kumar, M. V. Rao, M. Pal, *Bioorg. Med. Chem. Lett.* **2012**, *22*, 2186-2191.

24. N. Younghwa, *J. Pharm. Pharmacol.* **2009**, *61*, 707-712.

25. A. Naya, M. Ishikawa, K. Matsuda, K. Ohwaki, T. Saeki, K. Noguchi, N. Ohtake, *Bioorg. Med. Chem.* **2003**, *11*, 875-884.

26. H. Wang, L. Lu, S. Zhu, Y. Li, W. Cai, *Curr. Microbiol.* **2006**, *52*, 1-5.

27. G. S. Suresh Kumar, A. Antony Muthu Prabhu, P. G. Seethalashmi, N. Bhuvanesh, S. Kumaresan, *J. Mol. Struct.* **2014**, *1059*, 51–60.

28. L. W. Wang, J. J. Kang, I. J. Chen, C. M. Teng, C. N. Lin, *Bioorg. Med. Chem.* **2002**, *10*, 567-572.

29. M. A. Bhat, A. M. Naglah, S. A. Ansari, H. M. Tuwajiria, A. Dhfyan, *Molecules.* **2021**, *26*, 3667.

30. F. Zelefack, D. Guilet, N. Fabre, C. Bayet, S. Chevalley, S. Ngouela, B. N. Lenta, A. Valentin, E. Tsamo, M. G. Dijoux-Franca, *J Nat Prod.* **2009**, *72*, 954-957.

31. K. Chibale, M. Visser, D. Schalkwyk, P. J Smith, A. Saravanamuthu, A. H. Fairlamb, *Tetrahedron.* **2003**, *59*, 2289-2296.

32. M. Nisar, I. Ali, M. R. Shahb, A. Badshaha, M. Qayumc, H. Khand, I. Khand, S. Alia, *RSC Adv.* **2013**,*3*,21753-21758.

33. A. Chaudhary, J. M. Khurana. *Curr. Org. Synth.* **2018**, *15*, 341-369.

34. S. Tu , J. Zhou , Z. Lu , X. Deng , D. Shi, S. Wang, *Synth. Commun.* **2002**, *32*, 3063–3067.

35. B. Rajitha, B. Sunil Kumar, Y. Thirupathi Reddy, P. Narsimha Reddy, N. Sreenivasulu, *Tetrahedron Lett.* **2005**, *46*, 8691–8693.

36. F. Darviche, S. Balalaie, F. Chadgani, P. Salehi, *Synth. Commun.* **2007**, *37*, 1059.

37. C. W. Kuo, J. M. Fang, *Synth.Commun.* **2001**, *31*, 877-892.

38. N. Mulakayala, P.V.N.S. Murthy, D. Rambabu, M. Aeluri, R. Adepu, G. R. Krishna, C. M. Reddy, K.R.S. Prasad, M. Chaitanya, C. S. Kumar, M. V. Basaveswara Rao, M. Pal, *Bioorg. Med. Chem. Lett.* **2012**, *22*, 2186–2191.

39. L. R. Devi, L. V. Chanu, I. H. Chanu and O. M. Singh, *Asian J. Chem.* **2016**, *28*, 1528-1530.

40. A. Roy, S. Behera, P.H. Mazire, B. Kumari, A. Mandal, B. Purkait, P. Ghosh, P. Das, P. Das, *Parasitol. Int.* **2021**, *82*, 102287.

41. M. K. Singh, S. K. Bhaumik, S. Karmakar, J. Paul, S. Sawoo, H. K. Majumder, A. Roy, *Exp. Parasitol*. **2017**, *175*, 8-20.

42. V. U. Pawar, S. Ghosh, B. A. Chopade, V. S. Shinde, *Bioorg. Med. Chem. Lett.* **2010**, *20*, 7243-7245.

43. P. P. Lawande, V. A Sontakke, N. M. Kumbhar, T. R. Bhagwat, S. Ghosh, V. S. Shinde, *Bioorg. Med. Chem. Lett.* **2017**, *27*, 5291-5295.

44. V. S. Shinde, P. P. Lawande, V. A. Sontakke, A. Khan, *Carbohydr. Res.* **2020**, *498*, 108178.

45. V. A. Sontakke, P. P. Lawande, A. K. Kate, A. Khan, R. Joshi, A. A. Kumbhar, V. S. Shinde, *Org. Biomol. Chem.* **2016**, *14*, 4136-4145.

46. K. A Qureshi, M. I. Ibrahim Al Nasr, W. S Koko, T. A. Khan, M. Jaremko, S. Mahmood, M. Q. Fatmi, *Antibiotics Basel.* **2022**, *11*, 1206.

47. A. Gimeno, M. J. Ojeda-Montes, S. Tomás-Hernández, A. Cereto-Massagué, R. Beltrán-Debón, M. Mulero, G. Pujadas, S. Garcia-Vallvé, *Int. J. Mol. Sci.* **2019**, *20*, 1375.

48. R. D. Kamble, R. J. Meshram, S. V. Hese, R. A. More, S. S. Kamble, R. N. Gacche, B. S. Dawane, *Comput. Biol. Chem.* **2016**, *61*, 86-96.

49. T. K. Harris, A. S. Mildvan, *Proteins*. **1999**, *1535*, 275-282.

50. K. K. Patil, R. J. Meshram, S. H. Barage, R. N. Gacche, *3 Biotech.* **2019**, *9*, 47.

51. R. Huey, G. M. Morris, A. J. Olson, D. S. Goodsell, *J. Comput. Chem*. 2007. 28, 1145-1152.

52. G. M. Morris, R. Huey, W. Lindstrom, M. F. Sanner, R. K. Belew, D. S. Goodsell, A. J. Olson. *J Comput Chem.* **2009**, *30*, 2785-2791.

53. S. Dallakyan, A. J. Olson, *Methods Mol Biol*. **2015**, *1263*, 243-50.

54. J. D. Yesselman, D. J. Price, J. L. Knight, C. L. Brooks. *J. Comput. Chem.* **2012**, *33*, 189-202.

55. R. J. Meshram, K. T. Bagul, S. P. Pawnikar, S. H. Barage, B. S. Kolte, R. N. Gacche, *J. Biomol. Struct. Dyn.* **2020**, *38*, 1168-1184.

56. J. C. Phillips, D. J. Hardy, J. D. C. Maia, J. E. Stone, J. V. Ribeiro, R. C. Bernardi, R. Buch, G. Fiorin, J. Hénin, W. Jiang, R. McGreevy, M. C. R. Melo, B. K. Radak, R. D.

Skeel, A. Singharoy, Y. Wang, B. Roux, A. Aksimentiev, Z. Luthey-Schulten, L. V. Kalé, K. Schulten, C. Chipot, E. Tajkhorshid, *J. Chem. Phys.* **2020**, *153*, 44130.

57. J. P. Ryckaert, G. Ciccotti, H. J. C. Berendsen, *J. Comput. Phys.* **1977**, *23*, 327–341.
58. T. Darden, D. York, L. Pedersen. *J Chem. Phys.***1993,** *98*, 10089-10092.
59. W. G. Hoover, *Phys Rev A*. **1985,** *31*, 1695-1697.
60. G. J. Martyna, D. J. Tobias, M. L. Klein, *J Chem Phys.***1994**, *101*, 4177–4189.
61. S. E. Feller, Y. Zhang, R. W. Pastor, S. R. Brooks, *J Chem Phys.***1995**, *103*, 4613–4621.
62. H. Liu, T. Hou, *Bioinformatics*. **2016**, *32*, 2216-2218.

Declaration of interests

The authors declare that they have no known competing financial interests or personal relationships that could have appeared to influence the work reported in this paper.

63.

Author Credit Statement

Kamlesh Lodha: Organic Synthesis

Deepak Wavhal: Data Curating

Namdeo Bhujbal: Resources

Priyanka Mazire: *In vitro* analysis

Sneha Bhujbal: *In silico* analysis

Ashlesha Korde: Writing Original Draft

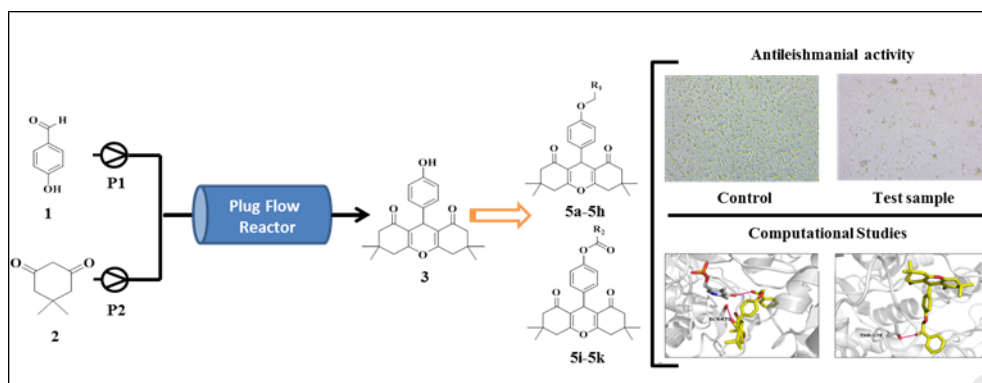Kamini Bagul: Writing, Review and Editing

Amit Roy: Validation of *in vitro* analysis

Rohan Meshram: Methodology, Validation of *in silico* analysis

Vaishali Shinde: Conceptualization, Supervision, Project administration

64.

Graphical Abstract

65.

Highlights

- Synthesized twelve 9-aryl-1,8-dioxo-octahydroxanthene derivatives.
- Continuous flow chemistry technique used for the synthesis of 9-aryl-1,8-dioxo-octahydroxanthene precursor.
- All the synthesized new molecules evaluated for their anti-leishmanial activity.
- Molecular dynamics simulation data presented here attempts to provide a structural and mechanistic explanation.

66.